CHALMERS
UNIVERSITY OF TECHNOLOGY

Low-Complexity Symbol Demapping for Multidimensional Multilevel Coded Modulation

Low-Complexity Symbol Demapping for Multidimensional Multilevel Coded Modulation

Tsuyoshi Yoshida[1,2], Koji Igarashi [2], Magnus Karlsson[3], and Erik Agrell[3]

[1] IT R&D Center, Mitsubishi Electric Corporation, Yoshida.Tsuyoshi@ah.MitsubishiElectric.co.jp
[2] Graduate School of Engineering, Osaka University
[3] Fiber Optic Communications Research Center (FORCE), Chalmers University of Technology

Abstract *Symbol demapping for multidimensional multilevel coding (MLC) is proposed, together with a novel nonsystematic encoding method, applicable to any dimensionality. The complexity of soft-decision forward error correction and symbol demapping, both normally problematic in multidimensional MLC, is reduced, which enables high-throughput implementation. ©2022 The Author(s)*

Introduction

Forward error correction (FEC) is an efficient tool for reliable communications, aiming for bit error rates (BER) down to 10^{-15}. There are several practical FEC schemes in fiber-optic communications: hard-decision (HD) FEC for direct-detection systems and 100 Gb/s coherent system [1,2], and soft-decision (SD) FEC for 400 Gb/s 16-ary quadrature amplitude modulation (QAM) systems [3,4]. SD-FEC additionally treats reliability information for better correction performance at the expense of larger complexity than HD-FEC [5]. Multilevel coding (MLC) [6] can ideally achieve the information-theoretic limits of multilevel systems, at the cost of a high SD-FEC complexity [7]. Methods for reducing the SD-FEC complexity in MLC were proposed in [8–15]. Probabilistic constellation shaping (PCS) is another key technique for approaching the capacity given by the Shannon limit [16]. Recent MLC techniques realized the combination of MLC with PCS [10,13–15,17].

While previous works [8–15] on MLC mainly focused on the complexity of SD-FEC coding, other functions, such as HD-FEC coding, symbol demapping, and (de)interleaving can also have significant complexities. Higher-dimensional MLC can further reduce the SD-FEC complexity at the expense of a larger dimension for the symbol demapping, a higher residual BER before HD-FEC decoding, and hence a higher HD-FEC redundancy.

This work aims at simplifying multidimensional (MD) MLC by introducing a simple symbol demapping, useful for channel-polarized (CP) MLC [14,15], and a nonsystematic (NS) MLC scheme, which is proposed here for the first time. Both are suitable for MD systems.

Principles

This section shows the principles for encoding and decoding, including the proposed symbol demapping functions for MLC with multistage decoding.

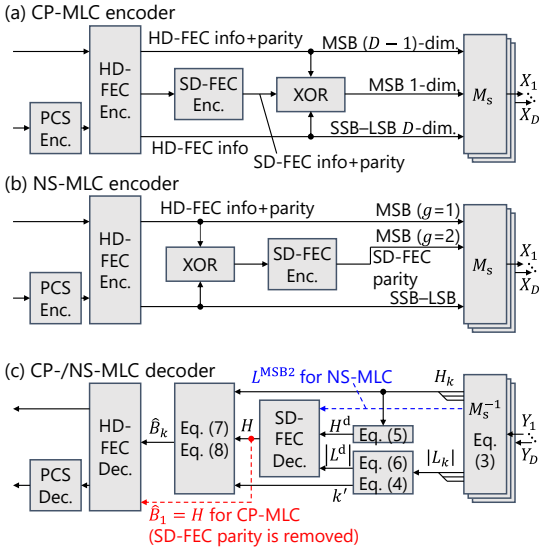

Fig. 1: Encoder and decoder blocks for CP-/NS-MLC.

Fig. 1 shows the FEC coding blocks for CP-MLC and NS-MLC, and Fig. 2 illustrates examples of the frame structures. The portion of the bit frame that controls the amplitudes of the channel-input symbols, i.e., the second-most to least significant bits (SSB–LSB) for a pulse amplitude modulation (PAM) symbol, is shaped in the PCS encoder. The PCS-encoded bits are then processed in either a CP-MLC or an NS-MLC encoder. Here, m_1 denotes the number of bit tributaries for a one-dimensional PAM symbol and D denotes the dimensionality of the MLC (i.e., the number of PAM symbols in the entire constellation set. Fig. 2 shows an example with $D = 2$ and $m_1 = 3$).

Fig. 1(a) is the encoder for CP-MLC [15]. The incoming bits are encoded by a systematic HD-FEC encoder and demultiplexed into $m = D \cdot m_1$ tributaries. All HD-FEC parity bits are placed on the sign-bit tributary (the most significant bit, MSB) for Gray-labelled PAM symbols. One of the sign-bit tributaries (the top row in Fig. 2) is further encoded by an SD-FEC encoder. An exclusive OR (XOR) operation among the m tributaries is

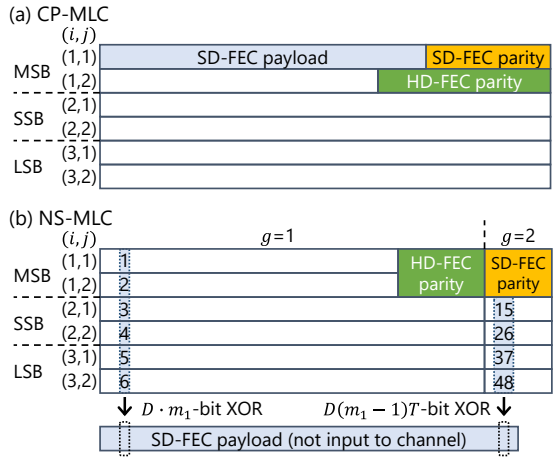

Fig. 2: Examples of frame structures ($D = 2$ and $m_1 = 3$): (a) CP-MLC and (b) NS-MLC ($T = 2$). Each PAM symbol is generated from the MSB, SSB, and LSB tributaries. NS-MLC has two symbol groups ($g \in \{1,2\}$).

then performed, which partitions the constellation set. The SD-FEC-encoded bits (including both payload and parity) are replaced by the XOR:ed bits. The obtained m bits are converted into channel-input MD symbols $\boldsymbol{X} = [X_1 X_2 \dots X_D]$ using a one-dimensional Gray encoder M_s independently for each 2^{m_1}-PAM symbol X_j; e.g., bits 000, 001, …, 111 are respectively converted into one-dimensional symbols 1, 3, 7, 5, –1, –3, –7, –5 if $m_1 = 3$. Here, $i \in \{1,2,\cdots,m_1\}$ denotes the bit tributary index for the PAM symbol in the j-th dimension ($j \in \{1,2,\cdots,D\}$), and the MD bit tributary index is $k = D(i-1) + j$.

Fig. 1(b) is the encoder for NS-MLC. One difference from the CP-MLC encoder is the location of the XOR operation, which is here placed before the SD-FEC encoding. The XOR:ed bits are encoded by the SD-FEC encoder. While the SD-FEC payload (systematic) bits are not used because they can be recovered from other bits at the decoder, the parity bits are fed to the symbol mapping. The other difference is that NS-MLC has two symbol groups, where $g \in \{1,2\}$ denotes the symbol group index. The symbol group 2 carries SD-FEC parity bits in MSB, while symbol group 1 does not. In symbol group 2 of NS-MLC, $D(m_1 - 1)T$ bits are XOR:ed, e.g., an 8-bit XOR is performed with $T = 2$ in Fig. 2(b).

The channel-output symbols $\boldsymbol{Y} = [Y_1 Y_2 \dots Y_D]$ should be softly demapped into a logarithmic ratio of *a posteriori* probabilities (*a posteriori* L-values) for the XOR:ed bits, i.e.,

$$L^{\text{ideal}} = \ln \frac{\sum_{\boldsymbol{x}\in\boldsymbol{\mathcal{X}}: b_{\text{xor}}=0} P_{\boldsymbol{X}}(\boldsymbol{x}) q_{\boldsymbol{X},\boldsymbol{Y}}(\boldsymbol{x},\boldsymbol{Y})}{\sum_{\boldsymbol{x}\in\boldsymbol{\mathcal{X}}: b_{\text{xor}}=1} P_{\boldsymbol{X}}(\boldsymbol{x}) q_{\boldsymbol{X},\boldsymbol{Y}}(\boldsymbol{x},\boldsymbol{Y})}, \quad (1)$$

where $P_{\boldsymbol{X}}(\boldsymbol{x})$, $q_{\boldsymbol{X},\boldsymbol{Y}}(\boldsymbol{x},\boldsymbol{y})$, and $\boldsymbol{\mathcal{X}}: b_{\text{xor}} = 0/1$ denote probability mass function of $\boldsymbol{X}$, decoding metric, e.g., $\exp(-\|\boldsymbol{y}-\boldsymbol{x}\|^2/(2\sigma^2))$ for an additive white Gaussian noise (AWGN) channel with a noise variance σ^2, and sets of partitioned MD constellations for the XOR:ed bit of 0/1, respectively. The L-values are processed by the SD-FEC decoder to yield decoded bits H. Bits input to the HD-FEC decoding are conventionally generated by hard-decision of $\boldsymbol{Y}$ based on H, i.e.,

$$\widehat{\boldsymbol{X}} = \underset{\boldsymbol{x}\in\boldsymbol{\mathcal{X}}: b_{\text{xor}}=H}{\arg\max}\ P_{\boldsymbol{X}}(\boldsymbol{x}) q_{\boldsymbol{X},\boldsymbol{Y}}(\boldsymbol{x},\boldsymbol{Y}). \quad (2)$$

The decided MD symbols $\widehat{\boldsymbol{X}}$ are demapped to bits $\hat{B}_k$. The decoding complexity of for the ideal symbol demapping rules (1) and (2) can however increase exponentially with D.

Fig. 1(c) is our decoder, including the proposed low-complexity symbol demapping functions based on the min-sum algorithm. The decoder can be almost identical for CP-MLC and NS-MLC. A channel-input PAM symbol for the j-th dimension, Y_j, is demapped into L-values

$$L^{\text{c}}_{i+jD} = \ln \frac{\sum_{x\in\boldsymbol{\mathcal{X}}: b_i=0} P_X(x) q_{X,Y}(x,Y_j)}{\sum_{x\in\boldsymbol{\mathcal{X}}: b_i=1} P_X(x) q_{X,Y}(x,Y_j)}. \quad (3)$$

The MD bit tributary with the smallest reliability,

$$k' = \underset{k}{\arg\min} |L^{\text{c}}_k|, \quad (4)$$

is identified, where $k = D(i-1) + j$. Then the sign and absolute value of the L-values,

$$H^{\text{d}} = \textstyle\sum_k H_k \bmod 2, \quad (5)$$

$$\left|L^{\text{d}}\right| = \left|L^{\text{c}}_{k'}\right|, \quad (6)$$

are respectively obtained, where $H_k \in \{0,1\}$ is the hard-decision bit of L^{c}_k, i.e., $H_k = 0$ if $L^{\text{c}}_k > 0$ and 1 otherwise. The SD-FEC decoder decodes the L-values $L^{\text{d}} = (-1)^{H^{\text{d}}}\left|L^{\text{d}}\right|$ into bits H. In symbol group 2 of NS-MLC, index k is given by $D(m_1 - 1)(t-1) + D(i-2) + j$ for $i \in \{2,3,\dots,m_1\}$, $j \in \{1,2,\dots,D\}$, and $t \in \{1,2,\dots,T\}$. The L-values for the SD-FEC parity bits (marked "MSB ($g = 2$)" in Fig. 1), L^{MSB2} (Fig. 1(c)), are directly fed to the SD-FEC decoding because they are not XOR:ed in the encoder. The HD-FEC decoder input bits $\hat{B}_k$ are then given by

$$\hat{B}_k = H_k \ \text{ if } \ k \neq k', \quad (7)$$

$$\hat{B}_{k'} = \left(H_k + H^{\text{d}} + H\right) \bmod 2. \quad (8)$$

These equations mean that only the least reliable bit is flipped, i.e., $\hat{B}_{k'} = \bar{H}_k$ if $H \neq H^{\text{d}}$. While $\hat{B}_1 = H$ for CP-MLC, H is not fed to the HD-FEC decoder for NS-MLC. The HD-FEC decoded bits are further processed in the PCS decoding before the frame termination. Note that the interleaver and deinterleaver are placed inside both SD-FEC and HD-FEC for breaking error bursts. The symbol demapping with (3)–(8) significantly reduces the complexity compared with the ideal demapper (1)–(2).

Simulations

Through numerical simulations over the AWGN channel, we verified the proposed low-complexity symbol demapping method and the proposed NS-MLC scheme. The performance degradation

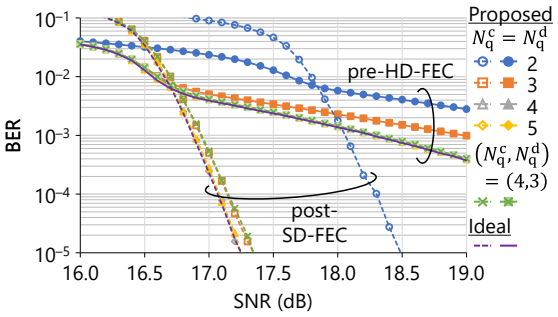

Fig. 3: Performance of the proposed symbol demapping for CP-MLC PCS-64-QAM ($D = 2$) with $N_q^c = N_q^d = 2{\sim}5$ or $(N_q^c, N_q^d) = (4,3)$ compared with ideal symbol demapping.

due to the quantization of the L-values L_k^c and L^d was characterized, as guidance for practical hardware implementation. As SD-FEC codes, the DVB-S2 low-density parity check codes [18] having a codeword length of 64800 and at most 10 decoding iterations were employed. The SD-FEC code rate for dimensionality $D = 1$, 2, or 4 was 2/3, 1/2, or 2/5 in CP-MLC and 3/4, 2/3, or 3/5 in NS-MLC, respectively. The probabilities of channel-input symbols were given by the Maxwell-Boltzmann distribution, and the two-dimensional entropy was 5.75 for PCS-64-QAM.

Fig. 3 shows the post-SD-FEC and pre-HD-FEC BER as a function of signal-to-noise ratio (SNR) for CP-MLC PCS-64-QAM with $D = 2$, for different quantization resolutions. The proposed symbol demapping with $(N_q^c, N_q^d) = (4,4)$, where N_q^c and N_q^d denote the number of quantization bits for L_k^c and L^d, respectively, showed negligible performance loss compared with ideal symbol demapping (1)–(2) with floating-point operations. The pre-HD-FEC BER displayed degraded waterfall and error floor performance for the proposed method with N_q^c and $N_q^d \leq 3$. If a slight loss in waterfall performance is acceptable, $(N_q^c, N_q^d) = (4,3)$ provides a reasonable performance–complexity tradeoff. Typical BER thresholds for use with HD-FEC codes are, e.g., $5{\times}10^{-3}$, $3{\times}10^{-3}$, and $5{\times}10^{-5}$ for 6.67%, 5%, and 1% overheads, respectively [19–21]. Setting $(N_q^c, N_q^d) = (4,3)$ or $(4,4)$, the required SNR was in both cases 17.3 dB for an HD-FEC overhead of 5% and a corresponding information rate of 4.99 bits per channel use (bpcu). The SNR gap to the Shannon limit was around 2.4 dB.

Fig. 4 shows the dependence on D for the same constellation as in Fig. 3 with CP-MLC and NS-MLC ($t = 1$). For each scheme and dimensionality, the assumed HD-FEC overhead, information rate, and SNR gap to the Shannon limit are shown. The quantization resolutions were $(N_q^c, N_q^d) = (4,3)$ or $(4,4)$. More bits for the quantization did not improve the pre-HD-FEC

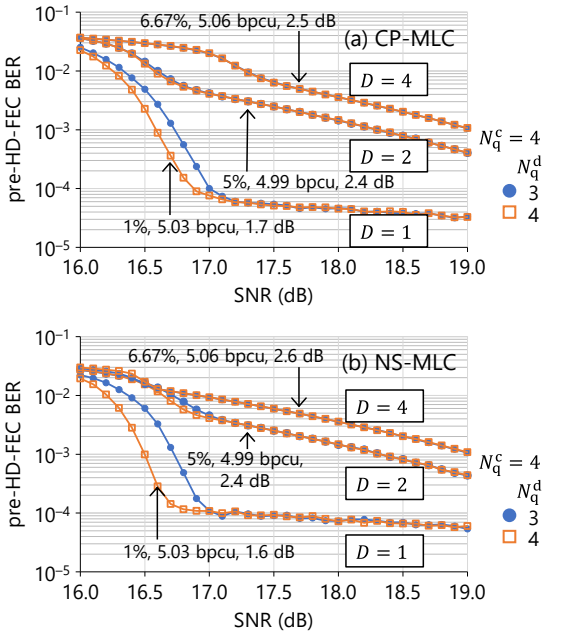

Fig. 4: Dependence on dimensionality D for PCS-64-QAM with (a) CP-MLC and (b) NS-MLC ($t = 1$), where $(N_q^c, N_q^d) = (4,3)$ or $(4,4)$. Assumed HD-FEC overhead, information rate, and SNR gap to the Shannon limit are described.

BER for $D \geq 2$. A higher D can reduce the SD-FEC complexity, but leads to a higher BER floor, requiring a higher redundancy in the HD-FEC for error-free operation, which results in a larger gap to the Shannon limit. The proposed symbol demapping worked well and the requirements for L-value quantization were similar for both MLC schemes. For lower-order QAM (not shown here) and lower D, the performance depends more strongly on the quantization resolution.

Conclusions

A low-complexity symbol demapping method for multidimensional MLC schemes was proposed. Through numerical simulations, satisfactory performance was confirmed for channel-polarized and the proposed nonsystematic MLC schemes, both combined with PCS. As guidance for practical DSP implementation, the dependence on the L-value quantization resolution was characterized, i.e., a good performance–complexity tradeoff was obtained with only 3- or 4-bit quantization.

Acknowledgements

This work is in part supported by National Institute of Information and Communications Technology (NICT), Japan.

References

[1] ITU-T, “Forward error correction for submarine systems,” recommendation G.975, 2000, [Online]. Available: https://www.itu.int/rec/T-REC-G.975

[2] B. P. Smith, A. Farhood, A. Hunt, F. R. Kschischang, and J. Lodge, “Staircase codes: FEC for 100 Gb/s OTN,” J. Lightw. Technol., vol. 30, no. 1, pp. 110–117, Jan. 2012, doi: 10.1109/JLT.2011.2175479.

[3] 400ZR, [Online]. Available: https://www.oiforum.com/technical-work/hot-topics/400zr-2

[4] Open ROADM MSA, [Online]. Available: www.openroadm.org/home.html

[5] F. Chang, K. Onohara, and T. Mizuochi, “Forward error correction for 100 G transport networks,” IEEE Commun. Mag., vol. 48, no. 3, pp. 548–555, Mar. 2010, doi: 10.1109/MCOM.2010.5434378.

[6] H. Imai and S. Hirakawa, “A new multilevel coding method using error-correcting codes,” IEEE Trans. Inf. Theory, vol. 23, no. 3, pp. 371–377, May 1977, doi: 10.1109/TIT.1977.1055718.

[7] U. Wachsmann, R. F. H. Fischer and J. B. Huber, “Multilevel codes: theoretical concepts and practical design rules,” IEEE Trans. Inf. Theory, vol. 45, no. 5, pp. 1361–1391, July 1999, doi: 10.1109/18.771140.

[8] A. Bisplinghoff, N. Beck, M. Ene, M. Danninger, and T. Kupfer, “Phase slip tolerant, low power, multi-level coding for 64QAM with 12.9 dB NCG,” in Proc. Opt. Fib. Commun. Conf. (OFC), Anaheim, CA, USA, Mar. 2016, Paper M3A.2, doi: 10.1364/OFC.2016.M3A.2.

[9] Y. Koganei, T. Oyama, K. Sugitani, H. Nakashima, and T. Hoshida, “Multilevel coding with spatially-coupled codes for beyond 400Gbps optical transmission,” in Proc. Opt. Fib. Commun. Conf. (OFC), San Diego, CA, USA, Mar. 2018, Paper Tu3C.2, doi: 10.1364/OFC.2018.Tu3C.2.

[10] K. Sugitani, Y. Koganei, T. Oyama, and H. Nakashima, “Partial multilevel coding with probabilistic shaping for low-power optical transmission,” in Proc. OptoElectron. Commun. Conf. (OECC), Fukuoka, Japan, July 2019, Paper TuB1-5, doi: DOI: 10.23919/PS.2019.8817878.

[11] F. Frey, S. Stern, J. K. Fischer, and R. F. H. Fischer, “Two-stage coded modulation for Hurwitz constellations in fiber-optical communications,” J. Lightw. Technol., vol. 38, no. 12, pp. 3135–3146, June 2020, doi: 10.1109/JLT.2020.2996365.

[12] M. Barakatain, D. Lentner, G. Böcherer, and F. R. Kschischang, “Performance-complexity tradeoffs of concatenated FEC for higher-order modulation,” J. Lightw. Technol., vol. 38, no. 11, pp. 2944–2953, June 2020, doi: 10.1109/JLT.2020.2983912.

[13] T. Yoshida, M. Karlsson, and E. Agrell, “Multilevel coding with flexible probabilistic shaping for rate-adaptive and low-power optical communications,” in Proc. Opt. Fib. Commun. Conf. (OFC), San Diego, CA, USA, Mar. 2020, Paper M3J.7, doi: 10.1364/OFC.2020.M3J.7.

[14] T. Kakizaki, M. Nakamura, F. Hamaoka, and Y. Kisaka, “Low-complexity channel polarized multilevel coding for modulation-format-independent forward error correction,” in Proc. Eur. Conf. Opt. Commun. (ECOC), Bordeaux, France, Sep. 2021, Paper Th1G.3, doi: 10.1109/ECOC52684.2021.9605828.

[15] T. Kakizaki, M. Nakamura, F. Hamaoka, and Y. Kisaka, “Low-complexity channel-polarized multilevel coding for probabilistic amplitude shaping,” in Proc. Opt. Fib. Commun. Conf. (OFC), San Diego, CA, USA, Paper W3H.4, doi: 10.1364/OFC.2022.W3H.4.

[16] G. Böcherer, F. Steiner, and P. Schulte, “Bandwidth efficient and rate-matched low-density parity-check coded modulation,” IEEE Trans. Commun., vol. 63, no. 12, pp. 4651-4665, Dec. 2015, doi: 10.1109/TCOMM.2015.2494016.

[17] L. Beygi, E. Agrell, J. M. Kahn and M. Karlsson, “Rate-adaptive coded modulation for fiber-optic communications,” J. Lightw. Technol., vol. 32, no. 2, pp. 333–343, Jan.15, 2014, doi: 10.1109/JLT.2013.2285672.

[18] European Telecommunications Standards Institute, Second generation framing structure, channel coding and modulation systems for broadcasting, interactive services, news gathering and other broadband satellite applications; Part 1 (DVB-S2), ETSI Standard EN 302 307-1 V1.4.1, Nov. 2014. [Online]. Available: www.dvb.org/standards

[19] L. M. Zhang and F. R. Kschischang, “Staircase Codes With 6% to 33% Overhead,” J. Lightw. Technol., vol. 32, no. 10, pp. 1999–2002, 15 May15, 2014, doi: 10.1109/JLT.2014.2316732.

[20] A. Y. Sukmadji, U. Martínez-Peñas and F. R. Kschischang, “Zipper Codes: Spatially-Coupled Product-Like Codes with Iterative Algebraic Decoding,” Canadian Workshop on Information Theory (CWIT), Hamilton, ON, Canada, June 2019, pp. 1-6, doi: 10.1109/CWIT.2019.8929906.

[21] D. S. Millar, R. Maher, D. Lavery, T. Koike-Akino, M. Pajovic, A. Alvarado, M. Paskov, K. Kojima, K. Parsons, B. C. Thomsen, S. J. Savory, and P. Bayvel, "Detection of a 1 Tb/s superchannel with a single coherent receiver," in Proc. Eur. Conf. Opt. Commun. (ECOC), Valencia, Spain, Sep.-Oct. 2015, Paper Mo.3.3.1, doi: 10.1109/ECOC.2015.7341618.